AN ANALYTIC APPROACH TO CHARACTERIZATION OF THE REMOTE FIELD EFFECT

Nathan Ida and Baiqiang Xu

Department of Electrical Engineering
The University of Akron
Akron, OH. 44325-3904

INTRODUCTION

The existing models for remote field testing are all based on the assumption that there are two domains for eddy current testing[1-3]. The first is a direct coupling domain. In this region, close to the driving coil, the fields obey the electromagnetic field equations. Fields are induced in all materials and, if the material is conducting, an induced eddy current distribution will exist. These eddy currents interact with any flaws that may exist to produce an indication in the testing instrument via any of the standard eddy current methods. A second domain is assumed to exist further away from the coil where direct induction is negligible. This is the indirect coupling domain. A flaw in this domain is detected by eddy currents that have presumably diffused to the outer surface of the test material, propagated on its outer surface and then propagated or diffused back into the material. While this model does explain the observed behavior in remote field testing it cannot explain some very simple situations. One is the testing of very thick materials. If a flaw is present near the inner surface of a tube with very thick walls (i.e. infinitely thick), the outer surface is very far away or does not exist and the existing models would predict no reading in the pickup coil. A second problem is the testing of nonconducting ferromagnetic materials like ferrites. These models indicate that such a material cannot be tested. Although, the remote field method is classified as an eddy current method, the same effect can be observed in nonconducting materials (i.e. the flux density in the remote field region is larger at larger distances from the axis of the coil). In addition, the use of numerical models based on a simplified form of Maxwell's equations, in which all propagating effects have been neglected, clearly shows the far field characteristics[4], indicating that wave propagation or guiding of waves by the metallic structure cannot be responsible for the effect.

The model presented here is based on an exact solution of the field equations in axisymmetric geometries and it clearly shows that the so called remote field effect is merely an extension to standard eddy current testing. The use of very low fields for detection is possible due to the unique field distribution of a coil and has nothing to do

Review of Progress in Quantitative Nondestructive Evaluation, Vol. 10A
Edited by D.O. Thompson and D.E. Chimenti, Plenum Press, New York, 1991

with the test material. For this reason the method can be applied to testing of nonconducting materials where the distortion in the field is detected. The present model also includes the effects of velocity of testing. The effect of velocity on the measured voltage is quite significant due to the low field intensity used.

THE MATHEMATICAL MODEL

The problem considered here has the geometry shown in Fig.1. A coil is moving with velocity v in the z direction inside a conducting tube of infinite length. The tube properties are defined by conductivity σ and permeability μ (the permeability of air is denoted by μ_0). The goal is to construct an analytic solution for the field induced by the exciting current density J in the coil.

A coordinate system which is moving with the coil is first established. Under this system,

$$\mathbf{B}=\mathbf{B}', \qquad \mathbf{E}=\mathbf{E}' + \mathbf{v} \times \mathbf{B} \tag{1}$$

where **B'**, and **E'** are the fields in a stationary reference frame. Introducing a magnetic vector potential **A** with Coulomb's gauge, namely, $\nabla\times\mathbf{A}=\mathbf{B}, \nabla\cdot\mathbf{A}=0$, into Maxwell's equation, the following governing equations are obtained:

$$\nabla^2\mathbf{A}+\mu_0\mathbf{J}=0 \quad \text{in air,} \quad \nabla^2\mathbf{A}-\mu\sigma\left(v\frac{\partial\mathbf{A}}{\partial z}+\frac{\partial\mathbf{A}}{\partial t}\right)=0 \quad \text{in tube} \tag{2}$$

For testing with the remote field effect Eq. (2) are written in cylindrical coordinates

$$\frac{1}{\rho}\frac{\partial}{\partial\rho}\left(\rho\frac{\partial A}{\partial\rho}\right)+\frac{\partial^2 A}{\partial z^2}-\frac{1}{\rho^2}A=-\mu_0 J \qquad \text{in air} \tag{3}$$

$$\frac{1}{\rho}\frac{\partial}{\partial\rho}\left(\rho\frac{\partial A}{\partial\rho}\right)+\frac{\partial^2 A}{\partial z^2}-\mu\sigma v\frac{\partial A}{\partial z}-\mu\sigma\frac{\partial A}{\partial t}-\frac{1}{\rho^2}A=\mathcal{L}A=0 \qquad \text{in tube} \tag{4}$$

where A denotes the ϕ component of the potential, and the operator $\mathcal{L}$ has been introduced to simplify expressions. The general problem in Eq. (3) and (4) can be modeled as

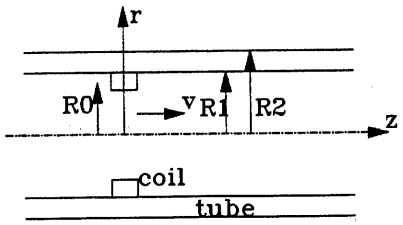

Figure 1. A general geometry used to develop the model.

$$\mathcal{L}A = -\mu_0 J \qquad (5)$$

with A bounded at $\rho=a$ and $\rho=\infty$. To solve the problem above, the following Green function problem is considered:

$$\mathcal{L}G = -\mu_0 \delta(\rho-\rho_0)\,\delta(z-z_0) \qquad (6)$$

with G bounded at $\rho=a$ and $\rho=\infty$. If J is uniformly distributed over an area Ω (i.e. cross section of a wire or coil) and G can be found, the solution to Eq. (5) can be written as

$$A = \int_{\Omega} JG(\rho-\rho_0, z-z_0)\,d\rho_0 dz_0 \qquad (7)$$

For the problem discussed, Ω is restricted to be inside the tube. Also, the current in the coil is assumed to be sinusoidal with frequency ω. This implies that the time dependency of potentials is $e^{i\omega t}$ and $A=\hat{A}e^{i\omega t}$. The governing equations are

$$\frac{1}{\rho}\frac{\partial}{\partial\rho}\left(\rho\frac{\partial\hat{A}}{\partial\rho}\right) + \frac{\partial^2\hat{A}}{\partial z^2} - \frac{1}{\rho^2}\hat{A} = -\mu_0\delta(\rho-\rho_0)\,\delta(z) \qquad \text{in air} \qquad (8)$$

$$\frac{1}{\rho}\frac{\partial}{\partial\rho}\left(\rho\frac{\partial\hat{A}}{\partial\rho}\right) + \frac{\partial^2\hat{A}}{\partial z^2} - \mu\sigma v\frac{\partial\hat{A}}{\partial z} - i\omega\mu\sigma\hat{A} - \frac{1}{\rho^2}\hat{A} = 0 \qquad \text{in tube} \qquad (9)$$

The Fourier transform with respect to z, is now taken

$$\frac{1}{\rho}\frac{\partial}{\partial\rho}\left(\rho\frac{\partial\tilde{A}}{\partial\rho}\right) - \left(\xi^2 + \frac{1}{\rho^2}\right)\tilde{A} = -\mu_0\delta(\rho-\rho_0) \qquad \text{in air} \qquad (10)$$

$$\frac{1}{\rho}\frac{\partial}{\partial\rho}\left(\rho\frac{\partial\tilde{A}}{\partial\rho}\right) - \left[\xi^2 + i\mu\sigma(\xi v+\omega) + \frac{1}{\rho^2}\right]\tilde{A} = 0 \qquad \text{in tube} \qquad (11)$$

where ξ is the transformed z coordinate and

$$\hat{A} = \frac{1}{2\pi}\int_{-\infty}^{+\infty}\tilde{A}e^{iz\xi}\,d\xi \qquad (12)$$

The general solutions to Eq. (10) and (11) are

$$\tilde{A} = aI_1(\xi\rho) + bK_1(\xi\rho) \text{ in air}, \quad \tilde{A} = cI_1(\zeta\rho) + dK_1(\zeta\rho) \text{ in tube} \qquad (13)$$

where a,b,c and d are constants to be evaluated and $\zeta^2=\xi^2+i\mu\sigma(\xi v+\omega)$

For the Green function solution the potential inside the tube is

$$\tilde{A}_1 = a_1 I_1(\xi\rho) \text{ for } \rho_0 \geq \rho, \qquad \tilde{A}_2 = c_1 I_1(\xi\rho) + a_2 K_1(\xi\rho) \text{ for } R_1 \geq \rho > \rho_0 \qquad (14)$$

The continuity and jump conditions at $\rho=\rho_0$ are

$$\tilde{A}_1 = \tilde{A}_2, \quad \frac{\partial \tilde{A}_2}{\partial \rho} - \frac{\partial \tilde{A}_1}{\partial \rho} = -\mu_0 \tag{15}$$

These conditions enable the evaluation of a_1, and a_2 as

$$a_1 = \mu_0 \rho_0 K_1(\xi\rho_0) + c_1, \qquad a_2 = \mu_0 \rho_0 I_1(\xi\rho_0) \tag{16}$$

The solutions in and outside the tube are

$$\tilde{A}_3 = c_2 I_1(\zeta\rho) + c_3 K_1(\zeta\rho) \text{ for } R_2 \geq \rho > R_1, \quad \tilde{A}_4 = c_4 K_1(\xi\rho) \text{ for } \rho > R_2 \tag{17}$$

The following interface conditions between air and material exist

$$\tilde{A}_2 = \tilde{A}_3, \quad \frac{1}{\mu_0}\frac{\partial}{\partial \rho}(\rho \tilde{A}_2) = \frac{1}{\mu}\frac{\partial}{\partial \rho}(\rho \tilde{A}_3) \qquad \text{at } \rho = R_1 \tag{18}$$

$$\tilde{A}_3 = \tilde{A}_4, \quad \frac{1}{\mu_0}\frac{\partial}{\partial \rho}(\rho \tilde{A}_4) = \frac{1}{\mu}\frac{\partial}{\partial \rho}(\rho \tilde{A}_3) \qquad \text{at } \rho = R_2 \tag{19}$$

A system of equations is established:

$$\begin{bmatrix} I_{1R_1} & -CI_{1R_1} & -CK_{1R_1} & 0 \\ \mu\xi R_1 I_{0R_1} & -\mu_0 \zeta R_1 CI_{0R_1} & \mu_0 \zeta R_1 CK_{0R_1} & 0 \\ 0 & CI_{1R_2} & CK_{1R_2} & -K_{1R_2} \\ 0 & \mu_0 \zeta R_2 CI_{0R_2} & -\mu_0 \zeta R_2 CK_{0R_2} & \mu\xi R_2 K_{0R_2} \end{bmatrix} \begin{bmatrix} C_1 \\ C_2 \\ C_3 \\ C_4 \end{bmatrix} = \begin{bmatrix} -\mu_0 \rho_0 I_{1\rho_0} K_{1R_1} \\ \mu\mu_0 \rho_0 \xi R_1 I_{1\rho_0} K_{0R_1} \\ 0 \\ 0 \end{bmatrix} \tag{20}$$

where $I_{nz} = I_n(\xi z)$, $K_{nz} = K_n(\xi z)$, $CI_{nz} = CI_n(\zeta z)$ and $CK_{nz} = CK_n(\zeta z)$. (20) leads to the solution of Eq. (10) and (11)):

$$\tilde{A}_1 = \mu_0 \rho_0 [K_1(\xi\rho_0) + \frac{P_1}{Q} I_1(\xi\rho_0)] I_1(\xi\rho) \qquad \rho_0 \geq \rho \tag{21}$$

$$\tilde{A}_2 = \mu_0 \rho_0 I_1(\xi\rho_0) [\frac{P_1}{Q} I_1(\xi\rho) + K_1(\xi\rho)] \qquad R_1 \geq \rho > \rho_0 \tag{22}$$

$$\tilde{A}_3 = \mu_0 \rho_0 I_1(\xi\rho_0) [\frac{P_2}{Q} I_1(\zeta\rho) + \frac{P_3}{Q} K_1(\zeta\rho)] \qquad R_2 \geq \rho > R_1 \tag{23}$$

$$\tilde{A}_4 = \mu_0 \rho_0 \frac{P_4}{Q} I_1(\xi\rho_0) K_1(\xi\rho) \qquad \rho > R_2 \tag{24}$$

where

$$P_1 = (\bar{\mu} CK_{1R_2} K_{0R_2} - \frac{\zeta}{\xi} K_{1R_2} CK_{0R_2})(\bar{\mu} CI_{1R_1} K_{0R_1} + \frac{\zeta}{\xi} K_{1R_1} CI_{0R_1}) - (\bar{\mu} CI_{1R_2} K_{0R_2} + \frac{\zeta}{\xi} K_{1R_2} CI_{0R_2})(\bar{\mu} CK_{1R_1} K_{0R_1} - \frac{\zeta}{\xi} K_{1R_1} CK_{0R_1}) \tag{25}$$

$$P_2 = \frac{\bar{\mu}}{\xi R_1}(\bar{\mu} CK_{1R_2} K_{0R_2} - \frac{\zeta}{\xi} K_{1R_2} CK_{0R_2}) \tag{26}$$

$$P_3 = \frac{\bar{\mu}}{\xi R_1}(\bar{\mu} CI_{1R_2} K_{0R_2} + \frac{\zeta}{\xi} K_{1R_2} CI_{0R_2}) \tag{27}$$

$$P_4 = -\frac{\bar{\mu}}{\xi^2 R_1 R_2} \tag{28}$$

$$Q=(\bar{\mu}CK_{1R_2}K_{0R_2}-\frac{\zeta}{\xi}K_{1R_2}CK_{0R_2})(\bar{\mu}CI_{1R_1}I_{0R_1}-\frac{\zeta}{\xi}I_{1R_1}CI_{0R_1})$$
$$-(\bar{\mu}CI_{1R_2}K_{0R_2}+\frac{\zeta}{\xi}K_{1R_2}CI_{0R_2})(\bar{\mu}CK_{1R_1}I_{0R_1}+\frac{\zeta}{\xi}I_{1R_1}CK_{0R_1}) \quad (29)$$

and $\bar{\mu}=\frac{\mu}{\mu_0}$ is the relative permeability of the material.

The Green function for the problem defined in Eq. (6), therefore, is

$$G=\frac{\mu_0\rho_0 e^{i\omega t}}{2\pi}\int_{-\infty}^{\infty}[FI_1(\chi\rho)+HK_1(\chi\rho)]e^{i\xi(z-z_0)}d\xi \quad (30)$$

where

$$F=\begin{cases} K_1(\xi\rho_0)+\frac{P_1}{Q}I_1(\xi\rho_0) \\ \frac{P_1}{Q}I_1(\xi\rho_0) \\ \frac{P_2}{Q}I_1(\xi\rho_0) \\ 0 \end{cases} \qquad H=\begin{cases} 0 & \rho_0\geq\rho \\ I_1(\xi\rho_0) & R_1\geq\rho>\rho_0 \\ \frac{P_3}{Q}I_1(\xi\rho_0) & R_2\geq\rho>R_1 \\ \frac{P_4}{Q}I_1(\xi\rho_0) & \rho>R_2 \end{cases} \quad (31)$$

and $$\chi=\begin{cases} \zeta & R_2\geq\rho>R_1 \\ \xi & \text{otherwise} \end{cases} \quad (32)$$

From Eq. (7) and (30), the solution to Eq. (5) may written as

$$A=Je^{i\omega t}\int_{r_1}^{r_2}d\rho_0\int_{z_{0a}}^{z_{0b}}dz_0\frac{1}{2\pi}\int_{-\infty}^{\infty}\mu_0\rho_0[FI_1(\chi\rho)+HK_1(\chi\rho)]e^{i\xi(z-z_0)}d\xi \quad (33)$$

Calculation of Flux Densities and Induced Voltage

Now **B** can be calculated from $\mathbf{B}=\nabla X\mathbf{A}$

$$B_\rho=-\frac{\partial A}{\partial z}, \qquad B_z=\rho\frac{\partial}{\partial\rho}(\rho A) \quad (34)$$

where B_ρ, B_z are the radial and axial components of the flux density.

To calculate the induced voltage V in an identical coil at $z=z_0$, the induced voltage in a loop of radius d inside the tube is first calculated

$$V_s=-\frac{\partial}{\partial t}\int_\sigma \mathbf{B}\cdot d\mathbf{s}=-i\omega\int_0^d \rho d\rho\int_0^{2\pi} B_z d\theta=-i2\pi\omega\int_0^d B_z\rho d\rho \qquad (35)$$

Performing integration over the coil cross sectional area, V is obtained as

$$V=-i2\pi n\omega\int_{r_1}^{r_2} dr\int_{z_0}^{z_0+a} dz\int_0^r B_z\rho d\rho \qquad (36)$$

where n is the turn density. This expression allows the calculation of the induced voltage in the pickup coil.

The expressions for the magnetic vector potential in Eq. (33) and subsequently those for B and V in Eq. (34) and (36) are quite complex and require considerable attention in evaluation, especially in conjunction with the far field effect. This is due to the need to evaluate the integrals at locations where the fields are very low. In addition, the integral in Eq. (33) can only be evaluated numerically, further complicating the calculation. However, with careful numerical evaluation, accurate results are obtained.

RESULTS AND DISCUSSION

The expressions above were used to model a number of geometries. The first of these is shown in Fig. 2. A single turn loop moves inside a bore in a conductor at a velocity v. The conductor is assumed to fill the whole space. Under these conditions, previous models cannot explain the detection of a defect either below the surface of the conductor or a surface breaking defect. The reason for this is that, if the idea of eddy currents difussing to the outer surface and then back is valid, then in this case, the field at the defect will be zero. However, for a given defect size and location, the field is almost independent of the thickness of the tube, clearly indicating a direct coupling rather than an indirect coupling as the existing models would predict. Fig. 3 shows the radial flux density at two locations below the surface of the bore. The deeper location has a larger field. This in turn indicates a higher sensitivity to a discontinuity at that location. In addition, the larger the distance between the two lines (L1 and L2), the larger the difference between the fields up to a point. Increasing the distance further, decreases the difference. This is true for the field of any finite length coil. The peak in the field occurs

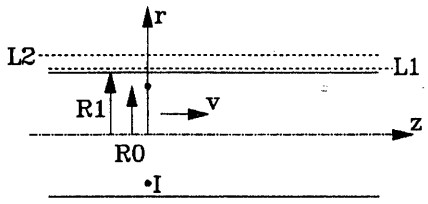

Figure 2. A loop moving in a bore. The rest of space is conducting.

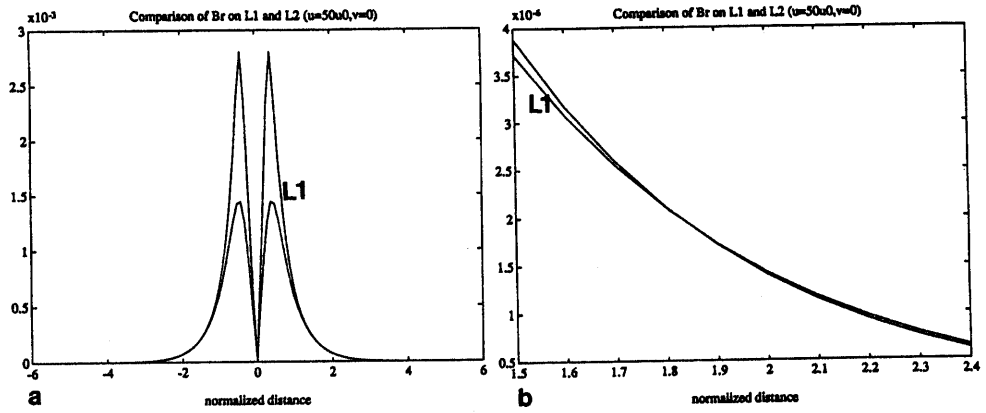

Figure 3. Radial component of flux density on line L1 and L2. a. comparison of fields, b. detail of flux densities in the remote field region.

at a larger radial distance away from the axis as the axial distance is increased. The domain where this occurs is the remote field domain.

A second geometry is a loop in air. The geometry is as in Fig. 2 but the permeability is set to μ_0 and the conductivity to zero. The remote field models currently in existance do not take this geometry into account. Yet, from Fig. 4, it is clear that the field at a larger distance is larger than the field at a smaller distance. If one were to locate any material at these two locations, the material at the larger distance will have a larger influence on the field. In effect, this indicates that the so called remote field effect exists in nonconducting materials, including free space. Since there are no eddy currents, the existing models fail. In fact, based on the existing models, testing of ferrites would not be possible because of their negligible conductivity. However, the fact that the same characteristics are observed with nonconducting materials suggests that the far field method should be applicable to nonconducting materials. In this case, the flaw indication is based on the distortion in the field due to the discontinuity in material properties.

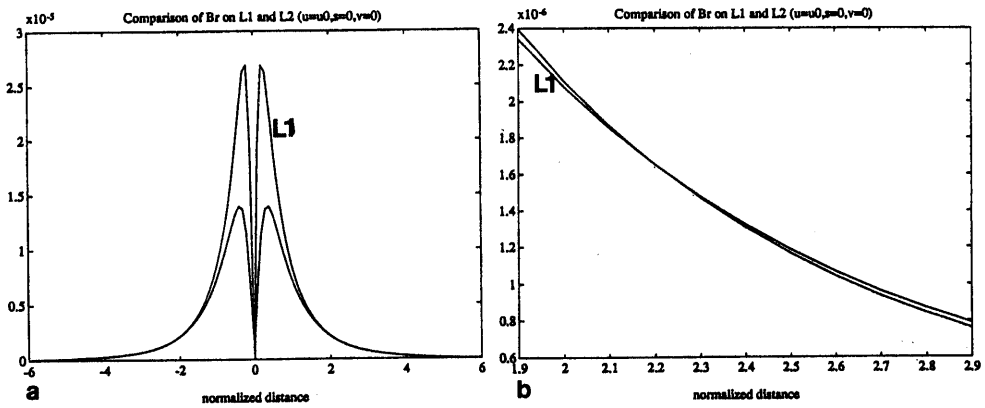

Figure 4. Radial component of flux density on line L1 and L2 for a loop in free space. a. comparison of fields, b. detail of flux densities in the remote field region.

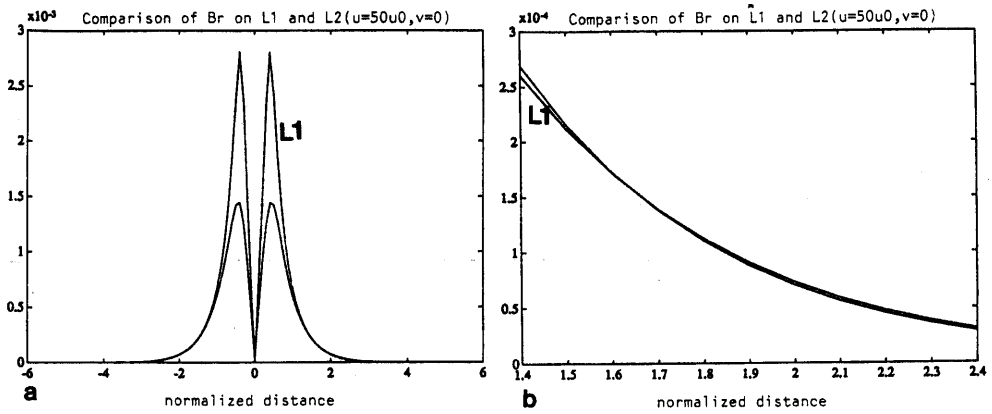

Figure 5. Radial component of flux density on line L1 and L2 for a coil in tube.
a. comparison of fields, b. detail of flux densities in the remote field region.

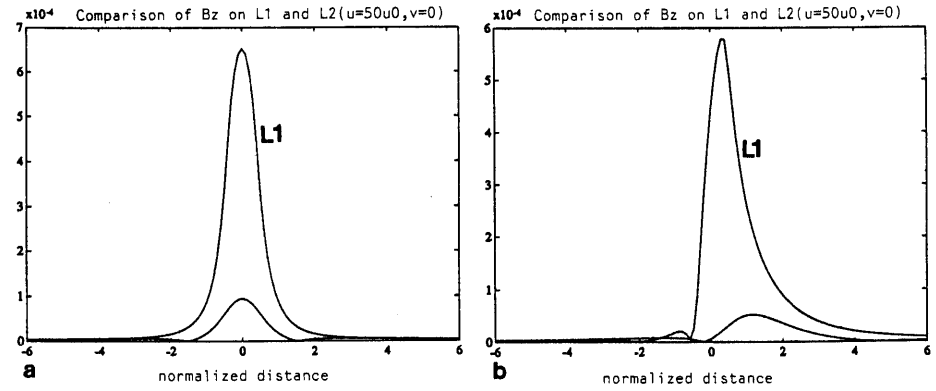

Figure 6. Effect of velocity on the axial component of flux density for a coil in tube.
a. stationary coil, b. v=10m/sec.

Fig. 5 shows the results for a thick ferromagnetic tube as in Fig. 1. This is the more common testing geometry, on which existing models are based.

Because the remote field testing method is based on low fields, the measured fields are quite sensitive to the velocity of testing. Fig. 6 shows comparison of the flux density at two velocities for a coil in a tube. In this case the axial component of the flux density is shown.

REFERENCES

1. T. R. Schmidt, Materials Evaluation, 42, 225, (1984).
2. D. L. Atherton, B. Stamm and S. Sulivan, Materials Evaluation, 44, 1544, (1986).
3. D. L. Atherton, B. Szpunar and S. Sulivan, Materials Evaluation, 45, 1083, (1987).
4. N. Ida, "The remote field effect and its interpretation", in Review of Progress in Quantitative Nondestructive Evaluation, D.O. Thompson and D.E. Chimenti, (Plenum Press, New York, 1989), Vol. 8a, p. 275.

Review of Progress in

QUANTITATIVE NONDESTRUCTIVE EVALUATION

Volume 10A